

Dry Micromanipulation of Supramolecular Giant Vesicles on a Silicon Substrate: Highly Stable Hydrogen-Bond-Directed Nanosheet Membrane

Hirotohi Sakaino,[†] Jun Sawayama,[†] Shin-ichiro Kabashima,^{†,‡} Isao Yoshikawa,[†] and Koji Araki^{*,†}

[†]Institute of Industrial Science, University of Tokyo, 4-6-1 Komaba, Meguro-ku, Tokyo 153-8505, Japan

[‡]Functional Materials Research Laboratories, Lion Corporation, 7-2-1 Hirai, Edogawa-ku, Tokyo 132-0035, Japan

S Supporting Information

ABSTRACT: Guanosine derivative **1** forms hydrogen-bond-directed giant vesicles. On a silicon substrate, the vesicles retain their shape and internal water phase even after removal of external water under vacuum. Dry manipulation of the micrometer-sized vesicles was carried out via AFM-tip-induced partition and fusion of the vesicles. For larger vesicles (5–10 μm), external solutions were successfully injected through a microcapillary inserted into the vesicle in air.

Micrometer-sized giant vesicles (GVs) of lipids and amphiphiles are attracting considerable interest as living-cell mimics and for their potential applications as microreactors or microcapsules for drug delivery.¹ However, the relatively poor stability of their structures is a major drawback for practical applications;² polymerized, polymer-supported, and block-copolymer amphiphiles have been studied to increase their stability.^{3–7} Amphiphilic compounds have both hydrophilic and hydrophobic units within the molecular structure. Hydrophobic interactions induce the aggregation of amphiphilic molecules in water to form self-assemblies of micelles, bilayer membranes, and other structures.⁸ Therefore, the vesicle membranes comprising lipids and amphiphiles are not sufficiently stable without an outer water phase, and vesicles that are stable in air are quite rare.⁹ We previously reported hydrogen-bond-directed giant multi- and unilamellar vesicles (GMVs and GUVs, respectively) of alkylsilylated guanosine derivative **1** (Figure 1a), which has a polar oxyethylene end group. Vesicle dispersions of **1** were conveniently prepared via the simple injection method,¹⁰ and the vesicles showed high stability and dispersibility in water. 2-D sheet assemblies with nanoscale thicknesses were formed through the interguanine 2-D hydrogen bond network (Figure 1b), one of the hydrogen bond motifs of guanine derivatives.¹¹ The vesicle surrounded by this membrane was very stable even when dry.

In this communication, we report the static and dynamic properties of the hydrogen bond-directed giant vesicles of **1**, which allow dry micromanipulation on a silicon substrate in the absence of an external aqueous phase. The femto- to picoliter-scale internal water phase inside of the vesicle is retained even when the vesicle is in vacuum. We demonstrate unprecedented AFM-tip-induced partitioning and fusion of the vesicles on a silicon substrate. Injection of external solutions and suction of

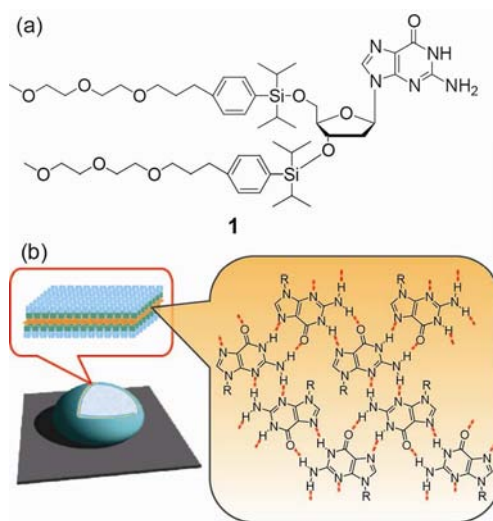


Figure 1. (a) Chemical structure and (b) 2-D hydrogen-bond-directed supramolecular vesicle of alkylsilylated guanosine derivative **1**.

the internal water through a microcapillary inserted into the vesicle are also presented. These results show the high static and dynamic stability of the nanometer-scale vesicle membrane assembled via the 2-D hydrogen bond network. As stable, nonvolatile, and processable microscale water pools¹² and microcapsules^{3–7} under dry conditions, these hydrogen-bond-directed supramolecular giant vesicles can be used in novel and unique applications such as microreactors, microcapsules for drug delivery, and microcontainers of denature-sensitive biomolecules.

Giant vesicles were prepared according to the previously reported procedure.¹⁰ Essentially, 0.1 mL of a THF solution of **1** ($2.50 \times 10^{-2} \text{ mol dm}^{-3}$) in the presence or absence of tetraethyleneglycol dodecyl ether (TEGDE; $2.50 \times 10^{-2} \text{ mol dm}^{-3}$) was mixed with 10 mL of pure water or aqueous fluorescence probe solution (eosin Y or FITC-Dex; $1.0 \times 10^{-5} \text{ mol dm}^{-3}$) to yield a translucent dispersion. Removal of TEGDE and the fluorescent probe in the external water phase via gel permeation chromatography (Sephadex G-25) gave the stable vesicle dispersion. Although the hydrogen bond interactions are not present in polar media,¹³ protection of

Received: July 24, 2012

Published: September 14, 2012

the hydrogen bonding site via rational molecular design enabled the formation of a hydrogen bond network even in a highly polar aqueous solution. The quantitative dispersion of **1** in water as spherical vesicles and the formation of the hydrogen-bond-directed 2-D sheet assemblies were confirmed via photometric quantification of **1**, optical microscopy, fluorescence microscopy, IR, and XRD. As reported previously,^{10b} the presence of TEGDE suppressed the formation of lamellar stacks of the hydrogen-bond-directed 2-D nanosheets; in aqueous dispersions, the vesicles were mostly GUVs with an average diameter of $1.73 \pm 0.58 \mu\text{m}$ surrounded by the 2.5-nm-thick nanosheet.

A drop of the vesicle solution with or without encapsulated fluorescence probe was placed on a silicon substrate. After drying *in vacuo* overnight, the vesicle on the substrate was observed via optical microscopy, confocal laser scanning microscopy (CLSM), and AC-mode atomic force microscopy (AFM). The AFM image showed that the average GUV diameter was $0.90 \pm 0.11 \mu\text{m}$ ($N = 46$) (Figure 2a). When

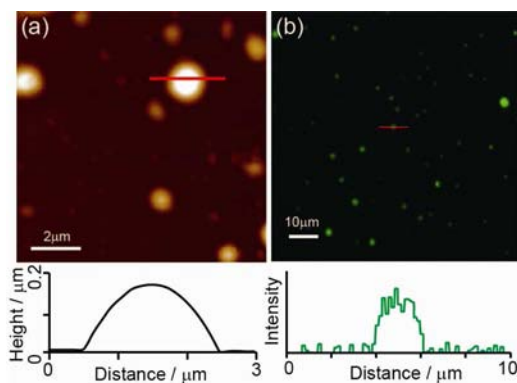


Figure 2. GUVs containing eosin Y deposited on a silicon substrate with subsequent vacuum drying. (a) AFM image (top) and height profile (bottom). (b) CLSM image (top) and the convex intensity profile along the red line (bottom).

vesicles smaller than the visible light wavelength were excluded, the average diameter became $1.57 \pm 0.13 \mu\text{m}$ ($N = 20$), which did not differ significantly from that in aqueous dispersion (Figure S1). The CLSM image was also similar to that of the GUVs in aqueous dispersion.¹⁰ The green fluorescence of the entrapped eosin Y (Figure 2b), which had a convex intensity profile, confirmed the presence of the internal water phase even after the removal of external water.¹⁴

A typical topographic image from AC-mode AFM is shown in Figure 2a together with the depth profile along the line, which revealed that the vesicles were flattened spheres $1.98 \mu\text{m}$ in diameter and $0.17 \mu\text{m}$ high. Although the AFM topographic image is not in clear focus, the sharp vesicle edge is evident in the phase image observation (Figure S2); this is presumably due to the highly deformable liquid-like nature of the vesicle.¹⁵

Figure 3a shows an AFM image of two initially separated spheroidal vesicles within a short distance of each other. Upon scanning with a silicon tip (Olympus silicon micro cantilever, OMCL-AC160TS-C2, radius = 6 nm, resonance frequency = 300 kHz, spring constant = 42 N m^{-1}) with high maximum force (15 nN) and speed ($110 \mu\text{m s}^{-1}$), the two spheroidal vesicles fused together into an elongated form (Figure 3b). No contraction of the vesicular size due to leakage of internal water was apparent, and the height remained at 380 nm. Further, the

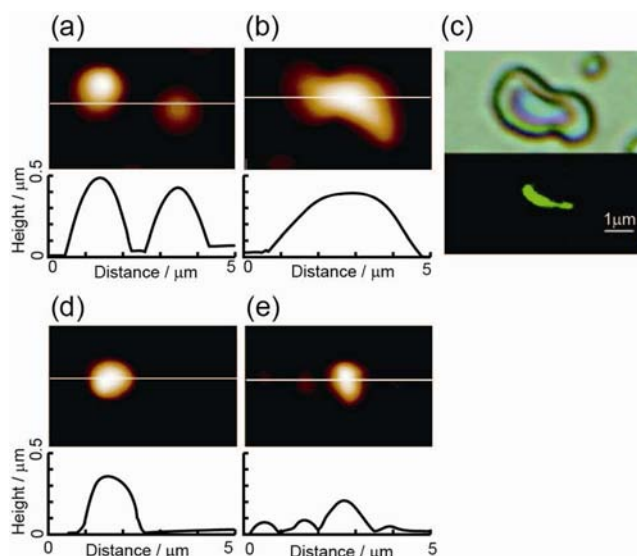


Figure 3. AFM-tip-induced fusion and partition of the vesicles on the substrate. AFM images (a) before and (b) after fusion. (c) Optical (top) and fluorescence (bottom) microscopy images after fusion. AFM images of the vesicle (d) before and (e) after partition.

fluorescence of the entrapped eosin Y in the two vesicles combined without fading. The fused vesicle on the substrate was subsequently kept under vacuum for a day, which did not significantly change the intensity of the green fluorescence of the encapsulated eosin Y (Figure 3c). These results confirm that there are no holes or defects in the vesicle membrane after fusion. In addition, partitioning of the vesicle into smaller vesicles (Figures 3d and 3e) was observed by scanning with a further increase in maximum force (20 nN) and scanning speed ($110 \mu\text{m s}^{-1}$). The observed response of the vesicles to the application of the shear by the AFM tip is similar to that of a macroscale water droplet on a solid surface, which suggests that the micrometer-scale giant vesicle surrounded by the nanometer-scale membrane does indeed have liquid-like properties.¹² When highly oriented pyrolytic graphite, which has a lower surface energy than silicon, was used as the substrate,¹⁶ scanning with increased maximum force resulted in displacement of the vesicles from their original position on the substrate but no vesicle partition. Since the surface of the 2-D nanosheet comprises polar oxyethylene groups, the adhesion imparted by polar interactions between the membrane surface of the vesicle and the substrate is thought to be important for the AFM-tip-induced micromanipulation. To the best of our knowledge, this is the first example of the fusion and partition of vesicles in the dry state, although the fusion of vesicles in solution has been studied extensively.^{17,18} The unprecedented AFM-tip-induced dry micromanipulation of the vesicles on a silicon substrate clearly demonstrates the unique properties of the 2-D hydrogen-bond-directed vesicle membranes including high stability, low water permeability, ability to retain encapsulated substances, and ability to undergo membrane fusion or partition under applied force due to the reversible nature of the intermolecular hydrogen bonds.

These GUVs on a silicon substrate have diameters of $\sim 1\text{--}2 \mu\text{m}$, which is too small to directly inject an external solution into the vesicle through a microcapillary.¹⁹ Accordingly, larger vesicles greater than $5 \mu\text{m}$ in diameter were prepared by slow injection of the **1**/THF solution without TEGDE. Appreciable

numbers of the larger vesicles were found on the substrate after subsequent drying in vacuum (Figure S3). The slow injection process might affect the stacking of preformed nanosheets in THF,¹⁰ allowing the formation of these larger vesicles. The membrane thickness of the larger vesicles ($>5 \mu\text{m}$) was estimated to be less than 100 nm by rupturing the vesicles via a slow freeze–thaw cycle and subsequent drying *in vacuo* (Figure S4). Therefore, the larger vesicles have a multilamellar membrane, whose thickness comprised less than 1/50 to 1/100 of the diameter of the vesicles. A microcapillary (Eppendorf Femtochips II) with inner and outer diameters of 0.5 and 0.7 μm , respectively, was used to manipulate the vesicles. As shown in Figure 4a and 4b, insertion and retraction

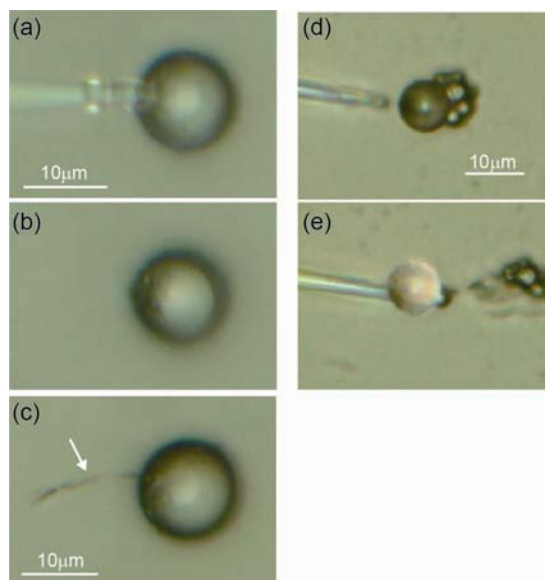


Figure 4. Dry manipulation of the vesicle on the silicone substrate. (a) Insertion of the tip into the vesicle. (b) Vesicle after insertion and retraction of the tip. (c) Horn-like extension of the membrane observed when the tip detached from the vesicle. (d, e) Lift and transport of the vesicle using the tip.

of the tip of the microcapillary caused negligible damage to the vesicles on the substrate in air: No leakage of internal water was observed, and the vesicle retained its 10 μm spherical shape throughout the process. On the other hand, internal water was quickly removed when the capillary was directly connected to a diaphragm-type aspirator (Figure S5). Occasionally, a horn- or tail-like extension of the membrane was observed when the tip detached from the vesicle (Figure 4c), but the vesicle itself remained intact. When the tip failed to penetrate the vesicle and instead slipped between the bottom of the vesicle and the substrate, the vesicle could be lifted onto the tip and carried elsewhere (Figure 4d and 4e). These results imply that the nanosheet membrane is highly deformable and rather adhesive.

Microinjection of aqueous eosin Y or FITC-Dex solution ($1.0 \times 10^{-5} \text{ mol dm}^{-3}$) to the inside of vesicles prepared in the absence of the fluorescent probe was attempted. A small amount of fluorescent probe solution was injected into the vesicle through the inserted tip of the microcapillary (Figure 5a). As a result, green fluorescence with a convex intensity profile was observed only at the vesicle (Figure 5b), which confirms the successful addition of the fluorescent probe to the internal water phase. After microinjection, the vesicle was maintained under vacuum for 2 h. Since no change in the green

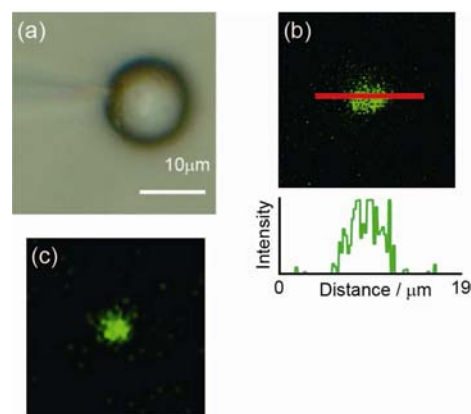


Figure 5. (a) Injection of FITC-Dex solution ($1.0 \times 10^{-5} \text{ mol dm}^{-3}$) into the vesicle through the inserted tip. (b) CLMS image (top) and convex intensity profile (bottom) of a vesicle after injection of the FITC-Dex solution into the internal water phase. (c) CLMS image of the vesicle after microinjection and subsequent vacuum drying (2 h).

fluorescence of low-molecular-weight eosin Y or high-molecular-weight FITC-Dex in the vesicle was observed even after vacuum drying (Figure 5c), it is evident that the nanosheet membrane completely self-healed after removal of the capillary tip; this ability is attributed to the flexible and reversible nature of the intermolecular hydrogen bonds.

Thus, the hydrogen-bond-directed 2-D nanosheet assembly of low-molecular-weight guanosine derivative **1** is shown to be soft and deformable, yet sufficiently stable against pressure differences in vacuum.²⁰ The high stability and reversible nature of the interguanine 2-D hydrogen bond networks endow the ability to deform and self-heal. Supramolecular giant vesicles comprising hydrogen-bond-directed 2-D nanosheet assemblies provide stable and nonvolatile femto- to picoliter-scale water pools even in vacuum. Fusion and partitioning of the water microdroplet and injection of external solutions can be achieved by dry manipulation via an external force and microcapillary, respectively. Since the vesicle can be handled in dry conditions, the internal water phase is not contaminated with the external liquid phase thereby providing a stable and unique microwater pool. We recently reported that hydrogen-bond-directed 2-D nanosheets of sulfamide derivatives are also sufficiently stable to form supramolecular gels and giant vesicles.²¹ Therefore, the remarkable properties observed in this study are not limited to guanosine derivative **1**. Other compounds that can form stable 2-D hydrogen bond networks could further contribute to the development of drug delivery systems, microreactors, and other applications.

■ ASSOCIATED CONTENT

Supporting Information

Full experimental details, synthesis of **2**, optical microscopy images, and AFM images. This material is available free of charge via the Internet at <http://pubs.acs.org>.

■ AUTHOR INFORMATION

Corresponding Author

araki@iis.u-tokyo.ac.jp

Notes

The authors declare no competing financial interest.

■ ACKNOWLEDGMENTS

This study is partly supported by a Grant-in-Aid for Challenging Exploratory Research (No. 21655038) from the Japan Society for the Promotion of Science (JSPS).

■ REFERENCES

- (1) (a) Karlsson, M.; Davidson, M.; Karlsson, R.; Karlsson, A.; Bergenholtz, J.; Konkoli, Z.; Jesorka, A.; Lobovkina, T.; Hurtig, J.; Voinova; Orwar, O. *Annu. Rev. Phys. Chem.* **2004**, *55*, 613–649. (b) Vriezema, D. M.; Aragonès, M. C.; Elemans, J. A. A. W.; Cornelissen, J. J. L. M.; Rowan, A. E.; Nolte, R. J. M. *Chem. Rev.* **2005**, *105*, 1445–1490. (c) Dimova, R.; Aranda, S.; Bezlyepkina, N.; Nikolov, V.; Riske, K. A.; Lipowsky, R. *J. Phys.: Condens. Matter* **2006**, *18*, S1151–S1176. (d) Christensen, S. M.; Stamou, D. *Soft Matter* **2007**, *3*, 828–836. (e) Kasuya, T.; Jung, J.; Kinoshita, R.; Goh, Y.; Matsuzaki, T.; Iijima, M.; Yoshimoto, N.; Tanizawa, K.; Kuroda, S. *Methods Enzymol.* **2009**, *464*, 147–166. (f) Walde, P.; Cosentino, K.; Engel, H.; Stano, P. *ChemBioChem* **2010**, *11*, 848–865.
- (2) Jesorka, A.; Orwar, O. *Annu. Rev. Anal. Chem.* **2008**, *1*, 801–832.
- (3) (a) Fukuda, H.; Diem, T.; Stefely, J.; Kezdy, F. J.; Regen, S. L. *J. Am. Chem. Soc.* **1986**, *108*, 2321–2327. (b) Ringsdorf, H.; Schlarb, B.; Venzmer, J. *Angew. Chem., Int. Ed. Engl.* **1988**, *27*, 113–158. (c) Chang, Z. L.; D’Ambruso, G. D.; Aspinwall, C. A. *Langmuir* **2006**, *22*, 9507–9511. (d) Zhang, H.; Joubert, J. R.; Saavedra, S. S. *Adv. Polym. Sci.* **2010**, *224*, 1–42.
- (4) (a) Aliev, K. V.; Ringsdorf, H.; Schlarb, B. *Makromol. Chem. Rapid Commun.* **1984**, *5*, 345–352. (b) Regen, S. L.; Shin, J.-S.; Yamaguchi, K. *J. Am. Chem. Soc.* **1984**, *106*, 2446–2447. (c) Purrucker, O.; Goennenwein, S.; Foertig, A.; Jordan, R.; Rusp, M.; Baermann, M.; Moroder, L.; Sackmann, E.; Tanaka, M. *Soft Matter* **2007**, *3*, 333–336.
- (5) (a) Jin, Y.; Qiao, Y.; Li, M.; Ai, P.; Hou, X. *Colloid Surf. B* **2005**, *42*, 45–51. (b) Iwamura, R.; Yoshida, K.; Masuda, M.; Yase, K.; Shimizu, T. *Chem. Mater.* **2002**, *14*, 3047–3053. (c) Mohanty, A.; Dey, J. *Langmuir* **2007**, *23*, 1033–1040. (d) Choi, B.; Kim, H.; Lee, B. I.; Lee, M. *Adv. Polym. Sci.* **2008**, *219*, 69–106.
- (6) van Dongen, S. F. M.; de Hoog, H.-P. M.; Peters, R. J. R. W.; Nallani, M.; Nolte, R. J. M.; van Hest, J. C. M. *Chem. Rev.* **2009**, *109*, 6212–6274.
- (7) (a) Discher, B. M.; Won, Y.-Y.; Ege, D. S.; Lee, J. C.-M.; Bates, F. S.; Discher, D. E.; Hammer, D. A. *Science* **1999**, *284*, 1143. (b) Discher, D. E.; Ahmed, F. *Annu. Rev. Biomed. Eng.* **2006**, *8*, 323–41. (c) Chen, Q.; Schoenherr, H.; Vancso, G. J. *Small* **2009**, *5*, 1436–1445.
- (8) *Self-Organized Surfactant Structures*; Tadros, T. F., Ed.; Wiley-VCH: Weinheim, Germany, 2010.
- (9) Homma, T.; Harano, K.; Isobe, H.; Nakaumura, E. *J. Am. Chem. Soc.* **2011**, *133*, 6364–6370.
- (10) (a) Sawayama, J.; Yoshikawa, I.; Araki, K. *Langmuir* **2010**, *26*, 8030–8035. (b) Sawayama, J.; Sakaino, H.; Kabashima, S.; Yoshikawa, I.; Araki, K. *Langmuir* **2011**, *27*, 8653–8658.
- (11) Lena, S.; Masiero, S.; Pieraccini, S.; Spada, G. P. *Chem.—Eur. J.* **2009**, *15*, 7792–7806.
- (12) (a) Meyer, E.; Mueller, M.; Braun, H.-G. *ACS Appl. Mater. Inter.* **2009**, *1*, 1682–1687. (b) Méndez-Vilas, A.; Jódar-Reyes, A. B.; González-Martín, M. L. *Small* **2009**, *5*, 1366–1390.
- (13) Jeffrey, G. A. *An Introduction to Hydrogen Bonding*; Oxford University Press: Oxford, 1997.
- (14) Bai, Z.; Lodge, T. P. *J. Am. Chem. Soc.* **2010**, *132*, 16265–16270.
- (15) (a) Chen, P.; Chen, L.; Han, D.; Zhai, J.; Zheng, Y.; Jiang, L. *Small* **2009**, *5*, 908–912. (b) Ko, J.-A.; Choi, H.-J.; Ha, M.-Y.; Hong, S.-D.; Yoon, H.-S. *Langmuir* **2010**, *26*, 9728–9735. (c) Tao, W.; Liu, Y.; Jiang, B.; Yu, S.; Huang, W.; Zhou, Y.; Yan, D. *J. Am. Chem. Soc.* **2012**, *134*, 762–764.
- (16) Mezey, L. Z.; Giber, J. *Jpn. J. Appl. Phys.* **1982**, *21*, 1569–1571.
- (17) Experimental: (a) Marsden, H. R.; Tomatsu, L.; Kros, A. *Chem. Soc. Rev.* **2011**, *40*, 1572–1585. (b) Sunami, T.; Caschera, F.; Morita, Y.; Toyota, T.; Nishimura, K.; Matsuura, T.; Suzuki, H.; Hanczyc, M. M.; Yomo, T. *Langmuir* **2010**, *26*, 15098–15103. (c) Ma, M.; Gong, Y.; Bong, D. *J. Am. Chem. Soc.* **2009**, *131*, 16919–16926. (d) Tanaka, T.; Yamazaki, M. *Langmuir* **2004**, *20*, 5160–5164. (e) Zhou, Y.; Yan, D. *J. Am. Chem. Soc.* **2005**, *127*, 10468–10469.
- (18) Theoretical: (a) Li, D.-W.; Liu, X. Y. *J. Chem. Phys.* **2005**, *122*, 174909. (b) Noguchi, H. *J. Phys. Soc. Jpn.* **2009**, *78*, 041007. (c) Shillcock, J.; Lipowsky, R. *Biophys. Rev. Lett.* **2007**, *2*, 33–55.
- (19) (a) Menger, F. M.; Gabrielson, K. D. *Angew. Chem., Int. Ed. Engl.* **1995**, *34*, 2091–2106. (b) Wick, R.; Angelova, M. I.; Walde, P.; Luisi, P. L. *Chem. Biol.* **1996**, *3*, 105–111. (c) Karlsson, M.; Nollkrantz, K.; Davidson, M. J.; Strömlberg, A.; Ryttsén, F.; Åkerman, B.; Orwar, O. *Anal. Chem.* **2000**, *72*, 5857–5862.
- (20) N-Acetylated derivative **2**, which cannot form the 2-D hydrogen bond network, was used as a control. Injection of a THF solution of acetylated derivative **2** in water only resulted in the formation of precipitates after standing for 1 day, confirming the essential role of the 2-D hydrogen bond network in the stable vesicles.
- (21) (a) Maeda, N.; Masuda, K.; Li, J.; Kabashima, S.; Yoshikawa, I.; Araki, K. *Soft Matter* **2010**, *6*, 5305–5307. (b) Kabashima, S.; Tanaka, S.; Kageyama, M.; Yoshikawa, I.; Araki, K. *Langmuir* **2011**, *27*, 8950–8955.